Imaging the Formation of High-Energy Dispersion Anomalies in the Actinide $UCoGa_5$

Tanmoy Das, Tomasz Durakiewicz, Jian-Xin Zhu, John J. Joyce, John L. Sarrao, and Matthias J. Graf

Theoretical Division, Los Alamos National Laboratory, Los Alamos, New Mexico 87545, USA

(Received 12 March 2012; revised manuscript received 5 June 2012; published 27 November 2012)

We use angle-resolved photoemission spectroscopy to image the emergence of substantial dispersion and spectral-weight anomalies in the electronic renormalization of the actinide compound $UCoGa_5$ that was presumed to belong to a conventional Fermi-liquid family. Kinks or abrupt breaks in the slope of the quasiparticle dispersion are detected both at low (approximately 130 meV) and high (approximately 1 eV) binding energies below the Fermi energy, ruling out any significant contribution of phonons. We perform numerical calculations to demonstrate that the anomalies are adequately described by coupling between itinerant fermions and spin fluctuations arising from the particle-hole continuum of the spin-orbit-split $5f$ states of uranium. These anomalies resemble the ''waterfall'' phenomenon of the high-temperature copper-oxide superconductors, suggesting that spin fluctuations are a generic route toward multiform electronic phases in correlated materials as different as high-temperature superconductors and actinides.

DOI: 10.1103/PhysRevX.2.041012 Subject Areas: Materials Science, Strongly Correlated Materials, Superconductivity

I. INTRODUCTION

The coupling between electrons and elementary excitations, originating from lattice or electronic degrees of freedom, can drive the formation of new emergent phases, such as magnetism and superconductivity. For rare-earth and actinide f-electron systems, the development of low-energy fermionic excitations with heavy electron mass is complicated by the interactions between f-electron spins and those of itinerant electrons. They often exhibit an interplay between Kondo physics, magnetism, and superconductivity [1]. So far, it has been thought that this physics is not at play in $UCoGa_5$ with a tetragonal crystal structure and metallic ground state [2]. In fact, it has been dubbed a *vegetable*, because of its lack of heavy mass [3,4], other competing orders [2,5–7], and showing of a spin-lattice relaxation rate that obeys the Korringa law of a conventional Fermi liquid at low temperatures [8]. However, at approximately 75 K, it violates the Korringa law by exhibiting a quadratic-temperature dependence without any sign of magnetic ordering. The simple lack of ordering is often contrasted with the rich properties of the isostructural $PuMGa_5$ and $PuCoIn_5$ compounds ($M = \mathrm{Co, Rh}$) [9]. Here, we show that $UCoGa_5$ is not a typical Fermi liquid. It is rather anomalous as evidenced by the drastic renormalization of the electronic dispersion at low and high binding energies when compared with *ab-initio* electronic bands. These kinks resemble the ''waterfall'' phenomenon of cuprates [10–12] and point toward a common mechanism of spin fluctuations in both d-and f-electron systems.

The actinide systems remain poised between the strong- and weak-coupling limit of Coulomb interaction. Therefore, they offer significant tunability across several correlated states of matter. The effective Coulomb repulsion U of the $5f$ electrons is not strong enough to localize all of them, yet it is sufficient to slow them down so they acquire a moderately increased mass near the Fermi level. The central puzzle is how this common low-lying heavy electronic state transforms into stable ground states that differ dramatically within the family [7,13,14]. An understanding of these differences hinges on knowing the nature of the exchanged bosons that dress the bare electrons to become heavy quasiparticles and ultimately drive the system into a particular stable ground state. The choice of $UCoGa_5$ for this study allows us to rule out any possible intervention of competing orders. Thus, it offers a clean approach to unravel the nature of the exchanged boson in the actinide family and related heavy-fermion systems.

II. EXPERIMENT

We use angle-resolved photoemission spectroscopy (ARPES) to image the momentum and energy dependence of the electronic dispersions and thereby reveal the renormalization of itinerant bands. Details of the ARPES experiments and calculations are described in the Supplementarl Material ([15], also see Refs. [16–25]). Figure 1 reports our main experimental result of $UCoGa_5$. A quick visual inspection of the spectral function in Figs. 1(a) and 1(b) (3D and 2D rendering of the same data, respectively) shows extensive spectral-weight redistribution both in momentum and energy space. The dispersion (traces of the intensity peaks) in Fig. 1(b) reveals a drastic departure of the quasiparticle states from the *ab-initio* electronic structure calculations (black dashed lines). More important, the

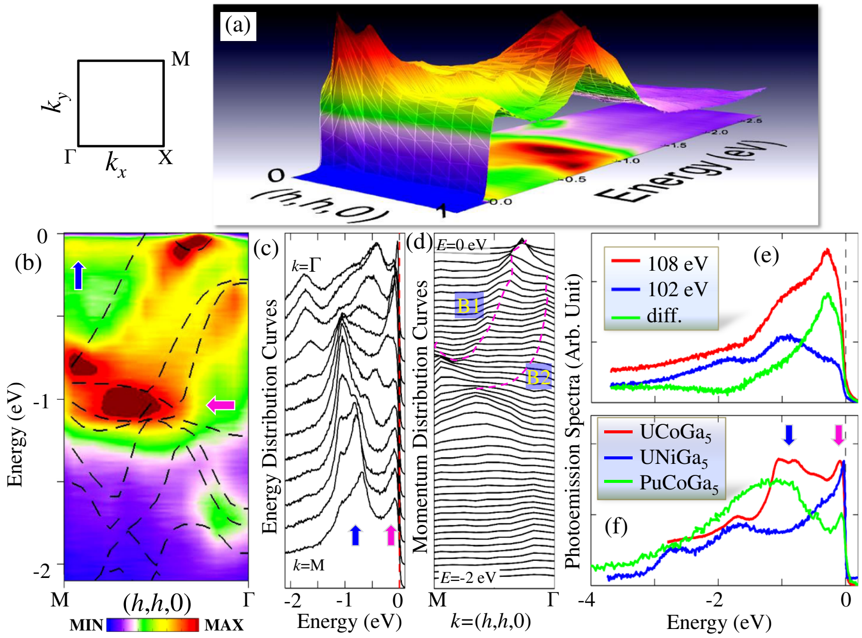

FIG. 1. Dispersion and measured ARPES spectral-function anomaly. (a) 3D intensity map of $UCoGa_5$ along the $M \rightarrow \Gamma$ direction $(h, h, 0)$ in the Brillouin zone. (b) Same data plotted as the 2D contour map and compared to the corresponding *ab-initio* GGA electronic band-structure dispersions (black dashed lines). Arrows indicate two quasi-non-dispersive energy scales of higher intensities. All the ARPES data are collected at the photon energy of 46 eV, with energy resolution better than 20 meV. (c) The EDCs are plotted for fixed momenta. The curves from bottom to top are chosen for equally spaced momentum points from M to Γ. The arrows have the same meaning as in panel (b). (d) MDCs for fixed binding energy. The bottom to top curves are chosen from $E = -2.1$ to $E = 0$ eV. The dashed lines are guide to the eyes for two extracted low-lying dispersions of anomalous character, analyzed in Fig. 2. (e) PES of $UCoGa_5$ at photon energies $h\nu = 108$ eV (red line) and $h\nu = 102$ eV (blue line). Their difference curve (green line) reveals the dominant $5f$ character [26]. (f) Partial PES of $UCoGa_5$ (momentum integrated between Γ and M) compared with two related actinides. $UNiGa_5$ and $PuCoGa_5$ exhibit antiferromagnetic [13] and superconducting [29] ground states, respectively. All data are normalized arbitrarily for ease of comparison.

associated quasiparticle width at the peak positions is significantly momentum and energy dependent. Unlike the renormalized quasiparticle-dispersion relation, which is a genuine manifestation of many-body correlation effects, the anomaly in the lifetime may have many intrinsic and extrinsic origins and is more difficult to assign to a particular mechanism [26] [see [15] on the extrinsic background]. We notice that while bare bands, computed within density functional theory based on a generalized gradient approximation (GGA), are present in the entire energy and momentum region, the spectral intensity is accumulated mainly at two energy scales. Such a connection between low- and high-energy scales is analogous to the so-called "waterfall" or high-energy-kink feature observed in single-band cuprates [10–12], where the band bottom lies at Γ, while here it is shifted to the M point.

The anomaly is markedly different in the energy and momentum space, which is a hallmark feature of correlated electron states. To expose this distinction, we present several energy-distribution curves (EDCs) of the ARPES intensity at several representative fixed momenta in Fig. 1(c), and momentum-distribution curves (MDCs) at several fixed energy points in Fig. 1(d). The peaks in the EDCs display prominent dispersionless features at two energy scales. The lowest energy peak persists at all momenta around −80 meV and gradually becomes sharper close to the Γ point. This low-energy feature reveals the formation of the long-lived renormalized quasiparticle. We will show below that the renormalization phenomena can be quantified to originate from the interaction of electrons with spin fluctuations, even without invoking the more traditional Kondo physics of heavy fermions. The high-energy feature around −1 eV is considerably broad in both energy and momentum space. In momentum space it attains a large width, demonstrating that these states are significantly incoherent. By comparing the experimental dispersion with its *ab-initio* counterpart, we can convincingly draw the conclusion that these incoherent states are created by spectral-weight depletion near −500 meV due to coupling to spin fluctuations. To gain further confidence about the correlation origin of these band anomalies, we note that such a redistribution of the spectral weight does not occur uniformly for the noninteracting bands; for instance, the spectral weight is strongly suppressed between −2 and −1.5 eV near the M point, albeit several bands are present in this part of the Brillouin zone. By comparing the

MDCs and EDCs, we immediately see that the spectrum is less dispersive as a function of momentum, while it disperses strongly with energy.

Figure 1(e) shows the quasiparticle peak pushed below the Fermi level by approximately 290 meV in the integrated photoemission spectrum (PES). The difference curve (green line) between measurements at 108 and 102 eV photon energies reveals that the quasiparticle states in the vicinity of the Fermi level are predominantly of a $5f$ character [26]. The partial PES that comes from the $\Gamma \rightarrow$ M momentum direction is obtained by integrating the spectrum in Fig. 1(b) and shown by the red line in Fig. 1(f). Interestingly, it displays a characteristic peak-dip-hump feature, which is generic for other isostructural actinides [6,27] (also shown here), as well as for δ-Pu [28] and copper-oxide superconductors [10–12] (not shown). Unlike $UCoGa_5$, the actinides $UNiGa_5$ and $PuCoGa_5$ exhibit antiferromagnetic [13] and superconducting [29] ground states, respectively.

III. ANALYSIS

In order to explain the correlation aspects of the dispersion anomalies, we extract two quasiparticle-dispersion branches by tracing the locii of the MDC peaks as shown in Fig. 2(a). To disentangle subtle features in the dispersion, the common practice is to observe the departure of the dispersion with respect to a featureless one ξ_{nk} (shown by dashed lines of the same color). A visual comparison reveals a sharp kink in the metallic actinide $UCoGa_5$, that is, a change in the slope of the dispersion. The low-energy kink lies around -130 meV (indicated by green arrow), which is higher than that in cuprates ($-$ 70 meV) [30]. On the other hand, the kink observed in the actinide USb_2 is at a much lower energy, and thus is most likely caused by electron-phonon coupling [31]. Furthermore, the high-energy kink of the waterfall ($-$ 1 eV) poses a ubiquitous anomaly as in cuprates [10–12]. On the basis of these comparisons, we deduce that the present kink lies well above the phonon energy scale of approximately 30 meV for metallic $UCoGa_5$ [32], and hitherto provides a novel platform to study the evolution of spin fluctuations in f-electron systems. It is known that the role of phonons vanishes in the high-energy scales of present interest in conventional metals, unlike, for example, in quasi-one-dimensional blue and red bronzes where the Peierls instability can shift the phonon energy scale by 10–15 times. [33,34].

In standard quantum field theory notation, the coupling between bosonic excitations and fermionic quasiparticles is defined by a complex fermionic self-energy $\Sigma_n(\boldsymbol{k}, \omega)$ function. The real and imaginary parts of the self-energy cause dispersion renormalization and quasiparticle-lifetime broadening, respectively. This information can be derived from the ARPES spectra by tracing the peak positions of the nth band $\boldsymbol{k}_n$ as

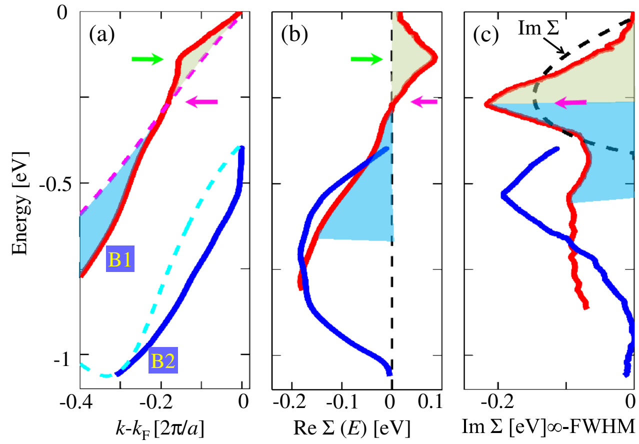

FIG. 2. The real and imaginary parts of the experimental self-energy. (a) Two low-lying dispersions derived from the peak positions of the MDCs [Fig. 1(d)] along M $\rightarrow \Gamma$. The momentum axis is offset by k_F for band B1. Dashed lines of same color give the *ab-initio* dispersion (offset from their corresponding Fermi-momenta values) which help expose the degree of anomaly for each dispersion with respect to their linear dispersion features. (b) The real part of the self-energy measures the deviation of each dispersion curve in panel (a) from its corresponding GGA value. The green arrow marks the location of the low-energy kink. (c) The inverse of the MDCs width obtained with the help of Fig. 1(c), which is proportional to the imaginary part of the self-energy, when the extrinsic background contribution is negligible. Different color fillings in all three curves (corresponding to band B1) separate the characteristic energy scale (marked by red arrows). The imaginary part attains a peak at the energy where the real part of the self-energy changes sign. To demonstrate this behavior we calculate ImΣ from ReΣ in panel (b) and plot it as a black dashed line in panel (c).

$$\mathrm{Re}\,\Sigma_n(\boldsymbol{k}, \omega) = \omega - \xi_{\boldsymbol{k},n}, \tag{1}$$

$$\mathrm{Im}\,\Sigma_n(\boldsymbol{k}, \omega) \propto 1/\mathrm{FWHM}_{\mathrm{MDC}}. \tag{2}$$

Here $\xi_{\boldsymbol{k},n}$ is the GGA dispersion with respect to its corresponding Fermi energy. The obtained results for ReΣ and the inverse full width at half maximum (FWHM) of MDC are given in Figs. 2(b) and 2(c), respectively, for the two extracted bands shown in Fig. 2(a). Taking advantage of our high-precision data, we expose two energy scales in ReΣ (marked by arrows) that are intrinsically linked to the quasiparticle lifetime $\tau = \hbar/(2\mathrm{Im}\Sigma)$. In addition to the peak at the kink energy, ReΣ possesses a sign reversal around 260 meV. This is an important feature that imposes the constraint that the corresponding ImΣ should yield a peak exactly at the same energy due to the Kramers-Kronig relationship. This is indeed in agreement with our findings for $UCoGa_5$ in Fig. 2(c), which exhibits a sharp peak in the extracted broadening, exactly where ReΣ changes sign (marked by a red arrow). It is worthwhile to mention that in ARPES measurements, the extrinsic source of quasiparticle broadening is typically known to be quasilinear in

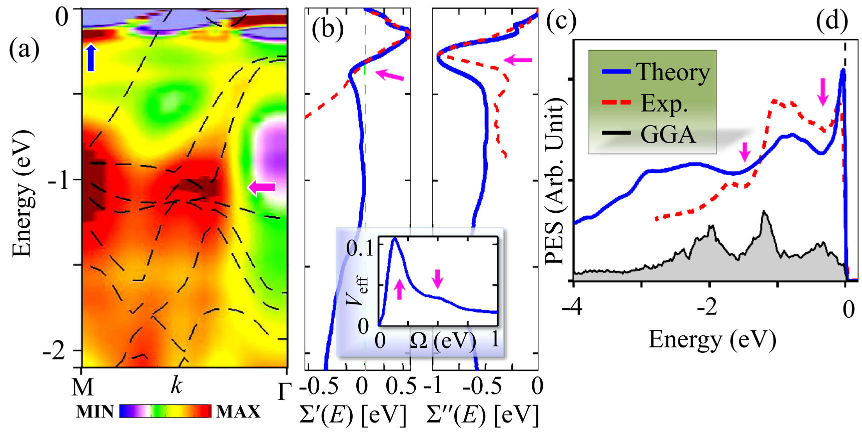

FIG. 3. Theoretical study of the spin-fluctuation-dressed dispersion anomaly. (a) Spectral-function intensity map versus energy and momentum along M → Γ. The black lines are the corresponding *ab-initio* bands. The arrows mark the two energy scales of highest intensity, as in Fig. 1(a). (b) The real part of the momentum and orbital averaged self-energy (blue line) compared with the experimental data (red dashed line). The experimental curve is multiplied by a factor of 5 for better visualization, because it is derived from a linear slope. The green dashed line marks the zero-energy axis. (c) The imaginary part of the self-energy shows a peak at the same energy where the experimental linewidth also has a peak. The inset shows the spin-fluctuation interaction potential responsible for the structures seen in the self-energy. (d) Computed partial PES (integrated over momentum between Γ and M) shows multiple peaks, as in the experimental curve [red dashed lines, taken from Fig. 1(e)]. The black line is the corresponding (normalized) GGA density of states. The red arrows mark the depletion of states, originating from the spin-fluctuation interaction.

energy [35], while the presence of a peak is a definitive signature of the intrinsic origin of broadening.

IV. NUMERICAL CALCULATIONS

Encouraged by the aforementioned analysis, we proceed with an *ab-initio* calculation to delineate the nature of the elementary excitations responsible for this anomaly. As mentioned before, both the energy scales and the strength of electron-phonon interaction [36,37] is insufficient to capture our observed dispersion anomalies. We demonstrate that the electron-electron interaction due to the dynamical spin fluctuations of exchanged bosons can describe the data. In $UCoGa_5$, strong spin-orbit coupling from relativistic effects enables substantial spin fluctuations whose feedback results in an increase of the electron mass and a shortening of the quasiparticle lifetime. We perform numerical calculations of the spin-fluctuation interaction potential (defined here as $V_{\rm eff}$) and resulting self-energy $\Sigma_n(\mathbf{k}, \omega)$ within spin-fluctuation coupling theory. Our intermediate coupling approach constrains the value of the Coulomb potential U to be of the order of the *ab-inito* band width ~1 eV; for details see [15].

The computed results are presented in Figs. 3(b) and 3(c). A close examination of all these spectra reveals essentially two energy scales tied to the electronic structure of $UCoGa_5$. In this system, the spin-orbit coupling of U atoms splits the degeneracy in the $5f$ states by approximately 500 meV [9], which stipulates a strong peak in $V_{\rm eff}$ and ImΣ (correspondingly ReΣ changes sign at this energy owing to the Kramers-Kronig relation). The second peak develops at a higher energy from the transition between unfilled $5f$ states and occupied $3d$ states of the Co atoms. Note that both energy scales are clearly discernible in $V_{\rm eff}$ (red arrows in the insert) and shift to higher energy in ImΣ due to the effects of dispersive bands. The peaks (dips) in ImΣ correspond to electronic spectral-weight dips (peaks) in ARPES as shown in Fig. 3(a). Importantly, the spin fluctuations also adequately explain the quasidispersionless renormalized feature around −80 meV and the spectral-weight peak-dip-hump features (marked by arrows), as observed in the ARPES spectra in Fig. 1(b), although some discrepancies exist. The momentum-integrated spectrum in Fig. 3(d) further demonstrates the presence of both dips in the experimental and theoretical spectra. We note that the calculated self-energy corrections only shift the GGA Fermi surface (FS) maps in the $k_z = 0$ plane. The computed FS maps are in accord with de Haas-van Alphen measurements, except for the tubelike FS around $(\pi/2, \pi/2, 0)$ [38]. Furthermore, our GGA calculation agrees with previous electronic structure calculations [36,37], except for the detailed shape of the tubelike FS. By turning on the self-energy, the disconnected tubelike FSs become connected along the k_z direction, as shown in the Supplemental Material [15], signaling a topological transition between a closed and open FS due to a small shift in Fermi energy.

Next we turn to estimating the degree of correlations in this material. The electron-phonon and spin-fluctuation coupling strength λ can be extracted from the slope of the self-energy in the low-energy region as $\mathrm{Re}\Sigma_n[\mathbf{k}, \xi_n(\mathbf{k}_F)] = -\lambda\xi_n(\mathbf{k}_F)$. Our theoretical estimate of the spin-fluctuation coupling constant is $\lambda_{\rm SF} = 1.0$. Experimentally, an estimate of λ at the Fermi level is obtained by comparing the measured Sommerfeld coefficient with respect to its noninteracting value $\gamma \approx (1 + \lambda)\gamma_0$. The reported measured values of γ are between $\gamma = 10$ and 21 $\mathrm{mJ/mol\,K^2}$ [5,7]. Our GGA calculated value of $\gamma_0 = 5.8$ $\mathrm{mJ/mol\,K^2}$ agrees well with the literature [36,37] and thus gives an experimental estimate of $\lambda_{\mathrm{exp}} \approx 0.7$–2.6. Therefore, the combination of spin fluctuations, $\lambda_{\mathrm{SF}} = 1.0$, and low-energy electron-phonon coupling, $\lambda_{\mathrm{ph}} \sim 0.7$ for $PuCoGa_5$ [32,39], adequately describes the observed electronic mass renormalization in $UCoGa_5$.

V. CONCLUSIONS

Our intermediate Coulomb-coupling approach offers an opportunity to address the complex nature of the dynamic band renormalization in actinides. This is not unexpected for materials with itinerant electrons, since similar theories based on the coupling between spin fluctuations and fermionic quasiparticles are among the leading contenders for explaining the origin of high-temperature superconductivity [40] and other emergent states of matter in d- and f-electron systems [41,42]. In addition, spin fluctuations in $5f$-electron systems are a manifestation of relativistic effects due to spin-orbit-split states of an order of approximately 500 meV in $UCoGa_5$. The emergence of a dispersionless band around -80 meV may be related to the breakdown of the Korringa law for the spin-lattice relaxation rate observed above approximately 75 K [8]. In fact, spin-orbit coupling may provide a novel electronic tunability for the interaction strength and characteristic frequency of the mediating boson. The results for the self-energy will motivate efforts to identify generic dispersion anomalies, waterfall physics, as well as their role on various mysterious spin-orbit-ordered emergent phases [14] in a larger class of actinide and heavy-fermion compounds.

ACKNOWLEDGMENTS

We thank A. V. Balatsky, F. Ronning, and E. D. Bauer for discussions. This work was supported by the U.S. Department of Energy (DOE) through the LANL LDRD Program (J.-X. Z. and M. J. G.) and the Office of Basic Energy Sciences, Division of Materials Sciences and Engineering (T. Das, T. D., J. J. J., and J. L. S.). Photoemission spectroscopy at the SRC is supported by the University of Wisconsin. Computations at the National Energy Research Scientific Computing Center (NERSC) is supported by the Office of Science of the U.S. DOE under Contract No. DE-AC02-05CH11231.

[1] A. C. Hewson, *The Kondo Problem to Heavy Fermions* (Cambridge University Press, Cambridge, 1983).

[2] Y. N. Grin, P. Rogl, K. Hiebl, *Structural Chemistry and Magnetic Behaviour of Ternary Uranium Gallides* U(Fe, Co, Ni, Ru, Rh, Pd, Os, Ir, Pt)Ga_5, J. Less-Common Met. **121**, 497 (1986).

[3] S. Ikeda, Y. Tokiwaa, T. Ōkuboa, M. Yamadaa, T. D. Matsudab, Y. Inadaa, R. Settaia, E. Yamamotob, Y. Hagab, and Y. Ōnukia, *Magnetic and Fermi Surface Properties of* $UTGa_5$ *(T: Fe, Co and Pt)*, Physica (Amsterdam) **329–333B**, 610 (2003).

[4] Y. Ōnuki, R. Settai, H. Shishido, S. Ikeda, T. D. Matsuda, E. Yamamoto, Y. Haga, D. Aoki, H. Harima, H. Harima, and H. Yamagami, *Fermi Surface Properties and Unconventional Superconductivity in Rare Earth, Uranium and Transuranium Compounds*, J. Optoelectron. Adv. Mater. **10**, 1535 (2008).

[5] S. Noguchi and K. Okuda, *Magnetism of Ternary Compounds U-T-Ga* (T = *Transition Elements)*, J. Magn. Magn. Mater. **104–107**, 57 (1992).

[6] T. Troć, Z. Bukowski, C. Sukowski, H. Misiorek, J. A. Morkowski, A. Szajek, and G. Chekowska, *Electronic Structure, Magnetic, and Transport Studies of Single-Crystalline* $UCoGa_5$, Phys. Rev. B **70**, 184443 (2004).

[7] N. O. Moreno, E. D. Bauer, J. L. Sarrao, M. F. Hundley, J. D. Thompson, and Z. Fisk, *Thermodynamic and Transport Properties of Single-Crystalline* $UMGa_5$ *(M =* Fe*, Co, Ni, Ru, Rh, Pd, Os, Ir, Pt)*, Phys. Rev. B **72**, 035119 (2005).

[8] S. Kambe, H. Sakai, H. Kato, Y. Tokunaga, T. Fujimoto, R. E. Walstedt, S. Ikeda, T. Maehira, Y. Haga, and Y. Onuki, *NMR Study of the Semimetallic Compound* $UCoGa_5$, Phys. Rev. B **76**, 024411 (2007).

[9] T. Das, J.-X. Zhu, M. J. Graf, *Spin Fluctuations and the Peak-Dip-Hump Feature in the Photoemission Spectrum of Actinides*, Phys. Rev. Lett. **108**, 017001 (2012).

[10] J. Graf, G.-H. Gweon, K. McElroy, S. Y. Zhou, C. Jozwiak, E. Rotenberg, A. Bill, T. Sasagawa, H. Eisaki, S. Uchida, H. Takagi, D.-H. Lee, and A. Lanzara, *Universal High Energy Anomaly in the Angle-Resolved Photoemission Spectra of High Temperature Superconductors: Possible Evidence of Spinon and Holon Branches.*, Phys. Rev. Lett. **98**, 067004 (2007).

[11] B. P. Xie, K. Yang, D. W. Shen, J. F. Zhao, H. W. Ou, J. Wei, S. Y. Gu, M. Arita, S. Qiao, H. Namatame, M. Taniguchi, N. Kaneko, H. Eisaki, Z. Q. Yang, and D. L. Feng, *High-Energy Scale Revival and Giant Kink in the Dispersion of a Cuprate Superconductor*, Phys. Rev. Lett. **98**, 147001 (2007).

[12] T. Valla, T. E. Kidd, W.-G. Yin, G. D. Gu, P. D. Johnson, Z.-H. Pan, and A. V. Fedorov, *High-Energy Kink Observed in the Electron Dispersion of High-Temperature Cuprate Superconductors*, Phys. Rev. Lett. **98**, 167003 (2007).

[13] K. Kanekoa, N. Metokia, G. H. Landera, N. Bernhoeftd, Y. Tokiwaa, Y. Hagaa, Y. Ōnukia, and Y. Ishii, *Neutron Diffraction Study of 5f Itinerant Antiferromagnet* $UPtGa_5$ *and* $UNiGa_5$, Physica (Amsterdam) **329–333B**, 510 (2003).

[14] T. Das, *Spin-Orbit Density Wave Induced Hidden Topological Order in* URu_2Si_2., Sci. Rep. **2**, 596 (2012).

[15] See Supplemental Material at http://link.aps.org/supplemental/10.1103/PhysRevX.2.041012 for technical details on the experiment, theory, and analysis.

[16] D. S. Inosov, J. Fink, A. A. Kordyuk, S. V. Borisenko, V. B. Zabolotnyy, R. Schuster, M. Knupfer, B. Bchner, R.

Follath, H. A. Drr, W. Eberhardt, V. Hinkov, B. Keimer, and H. Berger, *Momentum and Energy Dependence of the Anomalous High-Energy Dispersion in the Electronic Structure of High Temperature Superconductors* Phys. Rev. Lett. **99**, 237002 (2007).

[17] S. Basak, T. Das, H. Lin, J. Nieminen, M. Lindroos, R. S. Markiewicz, and A. Bansil, *Origin of the High-Energy Kink in the Photoemission Spectrum of the High-Temperature Superconductor* $Bi_2Sr_2CaCu_2O_8$, Phys. Rev. B **80**, 214520 (2009).

[18] H. Iwasawa, Y. Yoshida, I. Hase, K. Shimada, H. Namatame, M. Taniguchi, and Y. Aiura, *High-Energy Anomaly in the Band Dispersion of the Ruthenate Superconductor.* Phys. Rev. Lett. **109**, 066404 (2012).

[19] Q. Wang, Z. Sun, E. Rotenberg, H. Berger, H. Eisaki, Y. Aiura, and D. S. Dessau, *Energy-Dependent Scaling of Incoherent Spectral Weight and the Origin of the Waterfalls in High-Tc Cuprates*, http://arxiv.org/abs/0910.2787.

[20] P. Blaha *et al.*, *An Augmented Plane Wave + Local Orbitals Program for Calculating Crystal Properties* (Tech. Universität Wien, Austria, 2001).

[21] J. P. Perdew, S. Burke, M. Ernzerhof, *Generalized Gradient Approximation Made Simple*, Phys. Rev. Lett. **77**, 3865 (1996).

[22] J. Kuneš, P. Novák, R. Schmid, P. Blaha, and K. Schwarz, *Electronic Structure of fcc Th: Spin-Orbit Calculation with* $6p_{1/2}$ *Local Orbital Extension*, Phys. Rev. B **64**, 153102 (2001).

[23] T. Takimoto, T. Hotta, and K. Ueda, *Strong-Coupling Theory of Superconductivity in a Degenerate Hubbard Model*, Phys. Rev. B **69**, 104504 (2004).

[24] T. Das, A. V. Balatsky, *Two Energy Scales in the Magnetic Resonance Spectrum of Electron and Hole Doped Pnictide Superconductors*, Phys. Rev. Lett. **106**, 157004 (2011).

[25] N. E. Bickers, D. J. Scalapino, and S. R. White, *Conserving Approximations for Strongly Correlated Electron Systems: Bethe-Salpeter Equation and Dynamics for the Two-Dimensional Hubbard Model*, Phys. Rev. Lett. **62**, 961 (1989).

[26] J. J. Yeh and I. Lindau, *Atomic Subshell Photoionization Cross Sections and Asymmetry Parameters* $1 \leq Z \leq 103$, At. Data Nucl. Data Tables **32**, 1 (1985).

[27] J. Joyce, J. Wills, T. Durakiewicz, M. Butterfield, E. Guziewicz, J. Sarrao, L. Morales, A. Arko, and O. Eriksson, *et al.*, *Photoemission and the Electronic Structure of* $PuCoGa_5$, Phys. Rev. Lett. **91**, 176401 (2003).

[28] A. J. Arko, J. J. Joyce, L. Morales, J. Wills, J. Lashley, F. Wastin, and J. Rebizant, *Electronic Structure of* α*- and* δ*-Pu from Photoelectron Spectroscopy*, Phys. Rev. B **62**, 1773 (2000).

[29] N. J. Curro, T. Caldwell, E. D. Bauer, L. A. Morales, M. J. Graf, Y. Bang, A. V. Balatsky, J. D. Thompson, and J. L. Sarrao, *Unconventional Superconductivity in* $PuCoGa_5$, Nature (London) **434**, 622 (2005).

[30] A. Lanzara, P. V. Bogdanov, X. J. Zhou, S. A. Kellar, D. L. Feng, E. D. Lu, T. Yoshida, H. Eisaki, A. Fujimori, K. Kishio, J.-I. Shimoyama, T. Nodak, S. Uchidak, Z. Hussain, and Z.-X. Shen, *Evidence for Ubiquitous Strong Electron-Phonon Coupling in High-Temperature Superconductors*, Nature (London) **412**, 510 (2001).

[31] T. Durakiewicz, P. S. Riseborough, C. G. Olson, J. J. Joyce, E. Bauer, J. L. Sarrao, S. Elgazzar, P. M. Oppeneer, E. Guziewicz, D. P. Moore, M. T. Butterfield, and K. S. Graham, *Observation of a Kink in the Dispersion of f-Electrons*, Europhys. Lett. **84**, 37003 (2008).

[32] P. Piekarz, K. Parlinski, P. T. Jochym, A. M. Oleś, J. P. Sanchez, and J. Rebizant, *First-Principles Study of Phonon modes in* $PuCoGa_5$ *Superconductor*, Phys. Rev. B **72**, 014521 (2005).

[33] S. Mitrovic, L. Perfetti, C. Sndergaard, G. Margaritondo, M. Grioni, N. Barisi, and L. Forró, *Electronic structure of a Quasi-One-Dimensional Insulator: The Molybdenum Red Bronze* $K_{0.33}Mn_{03}$, Phys. Rev. B **69**, 035102 (2004).

[34] M. Grioni, S. Pons, and E. Frantzeskakis, *Recent ARPES Experiments on Quasi-1D Bulk Materials and Artificial Structures*, J. Phys. Condens. Matter **21**, 023201 (2009).

[35] D. A. Shirley, *High-Resolution X-Ray Photoemission Spectrum of the Valence Bands of Gold*, Phys. Rev. B **5**, 4709 (1972).

[36] T. Maehira, T. Hotta, K. Ueda, and A. Hasegawa, *Electronic Structure and the Fermi Surface of* $PuCoGa_5$ *and* $NpCoGa_5$, Phys. Rev. Lett. **90**, 207007 (2003).

[37] I. Opahle, S. Elgazzar, K. Koepernik, and P. M. Oppeneer, *Electronic Structure of the Pu-Based Superconductor* $PuCoGa_5$ *and of Related Actinide-115 Compounds*, Phys. Rev. B **70**, 104504 (2004).

[38] S. Ikeda, Y. Tokiwa, T. Okubo, Y. Haga, E. Yamamoto, Y. Inada, R. Settai, and Y. Ōnuki, *Magnetic and Fermi Surface Properties of* $UCoGa_5$ *and* $URhGa_5$., J. Nucl. Sci. Technol., Suppl. **3**, 206 (2002).

[39] N. Metoki, K. Kaneko, S. Raymond, J.-P. Sanchez, P. Piekarz, K. Parlinski, A. M. Oleś, S. Ikeda, T. D. Matsuda, Y. Haga, Y. Onuki, and G. H. Lander, *Phonons in* $UCoGa_5$, Physica (Amsterdam) **378–380B**, 1003 (2006).

[40] D. J. Scalapino, E. Loh, and J. E. Hirsch, *d-Wave Pairing Near a Spin-Density-Wave Instability*, Phys. Rev. B **34**, 8190 (1986).

[41] T. Moriya and T. Takimoto, *Anomalous Properties around Magnetic Instability in Heavy-Electron Systems*, J. Phys. Soc. Jpn. **64**, 960 (1995).

[42] T. Moriya, *Spin fluctuations in Itinerant Electron Magnetism* (Springer, Berlin, 1985).